arXiv:1302.0150v2 [hep-lat] 7 Feb 2013

February 2013

Monte Carlo Study of Strongly-Interacting Degenerate Fermions: a Model for Voltage-Biased Bilayer Graphene

Wes Armour[a], **Simon Hands**[b] **and Costas Strouthos**[c]

[a] *Oxford e-Research Centre, University of Oxford, 7 Keble Road, Oxford OX1 3QG, United Kingdom.*

[b] *Department of Physics, College of Science, Swansea University, Singleton Park, Swansea SA2 8PP, United Kingdom.*

[c] *Computation-based Science and Technology Research Center, The Cyprus Institute, 1645 Nicosia, Cyprus.*

Abstract: We formulate a model of $N_f = 4$ flavors of relativistic fermion in 2+1d in the presence of a chemical potential μ coupled to two flavor doublets with opposite sign, akin to isopsin chemical potential in QCD. This is argued to be an effective theory for low energy electronic excitations in bilayer graphene, in which an applied voltage between the layers ensures equal populations of particles on one layer and holes on the other. The model is then reformulated on a spacetime lattice using staggered fermions, and in the absence of a sign problem, simulated using an orthodox hybrid Monte Carlo algorithm. With the coupling strength chosen to be close to a quantum critical point believed to exist for $N_f < N_{fc} \approx 4.8$, it is found that there is a region below saturation where both the carrier density and a particle-hole "excitonic" condensate scale anomalously with increasing μ, much more rapidly that the corresponding quantities in free field theory, while the conventional chiral condensate is strongly suppressed. The corresponding ground state is speculated to be a strongly-correlated degenerate fermion system, with a remnant Fermi surface distorted by a superfluid excitonic condensate. The model thus shows qualitatively different behaviour to any model with $\mu \neq 0$ previously studied by lattice simulation.

Keywords: graphene, lattice simulation, quantum critical point, chemical potential

1 Introduction

The study of quantum systems containing a non-zero density of conserved charge beyond perturbation theory remains a challenging but fascinating problem. Estimating Euclidean Green functions via Monte Carlo importance sampling of the discretised path integral is rendered inoperable once $\mu/T \gg 1$, where μ is the chemical potential associated with the conserved charge such that the charge density $n = \partial \ln \mathcal{Z}/\partial\mu$, because generically the integrand $e^{-S_E(\mu)}$, with S_E the action in Euclidean metric, is not positive definite once $\mu \neq 0$. There remain a small number of interesting problems with real S_E which can be tackled by orthodox methods: fermionic models such as Gross-Neveu and NJL, which with $\mu \neq 0$ are either Fermi liquids [1] or weakly-interacting BCS superfluids [2, 3]; certain gauge theories with groups such as SU(2) [4] or G_2 [5] containing real matter representations; and QCD with non zero isospin density [6]. There is also a recent study of the interacting relativistic Bose gas which deals with a complex S_E by sampling a complexified configuration space using Langevin dynamics [7].

In the present paper we claim to add to this list a model of strongly-interacting fermions in 2+1d inspired by recent developments in graphene. Recall that due to the special properties of the honeycomb lattice (with just two isolated zeros or "Dirac points" of the dispersion $E(\vec{k})$ in the first Brillouin zone), low energy excitations of either electron or hole nature are naturally described by a 2+1d Dirac equation. For monolayer graphene, the counting of degrees of freedom (2 Dirac points $\times$ 2 C atoms per unit cell $\times$ 2 electron spin components) results in $N_f = 2$ flavors of 4-component relativistic spinor fields. Here we consider a model of bilayer graphene comprising $N_f = 4$ relativistic flavors, in which a biassing voltage is applied across the layers so that a non-zero density of electrons is induced on the negative sheet and an equal density of holes induced on the positive. It will be shown in Sec. 2 that this is equivalent to introducing an equal and opposite chemical potential μ on each sheet, so that the resulting relativistic effective theory has an "isospin" chemical potential μ_I with two "u" and two "d" flavors. Just as for QCD, it is straightforward to show the resulting S_E is real and positive so that Monte Carlo simulation is applicable.

The role for numerical simulation becomes apparent once inter-electron interactions are considered. The Coulomb interaction between charges in graphene is effectively enhanced by a factor $v_F/c \approx 300$, where $v_F = \partial E/\partial k|_{k=k_F}$ is the Fermi velocity of the charge carriers, which is constant for a linear dispersion. Since in undoped graphene with carrier density $n_c = 0$ only quantum fluctuation (namely vacuum polarisation) effects contribute to screening, the resulting effective theory of relativistic electrons has an effective fine structure constant $\alpha_{\text{eff}} \sim O(1)$, albeit with a non-covariant "instantaneous" interaction of the form $A_0\bar{\psi}\gamma_0\psi$ due to $v_F \ll c$. This implies that the theory must be treated as strongly-interacting, and the possibility of non-perturbative effects such as particle-hole condensation $\langle\bar{\psi}\psi\rangle \neq 0$, resembling chiral symmetry breaking and resulting in dynamical mass gap generation leading to a Mott insulator phase, should be considered. Son [8], in the context of a model with N_f relativistic species and variable coupling strength α has suggested that gap generation occurs for N_f sufficiently

small and α suffciently large. Moreover, the critical coupling $\alpha_c(N_f)$ defines a quantum critical point (QCP) where the scaling of operators and correlation functions in principle receive anomalous corrections, which could for instance modify the linearity of the electron dispersion.

The scenario was tested in a Monte Carlo simulation with $2{+}1d$ staggered fermions (at a QCP the underlying lattice should become irrelevant) [9]; in the strong coupling limit $\alpha \to \infty$ the QCP is found for $N_{fc} = 4.8(2)$. Simulations incorporating a more realistic long-ranged Coulomb interaction estimated $\alpha_c = 1.11(6)$ [10] for the case $N_f = 2$ relevant for monolayer graphene, suggesting there is a real possibility of gap generation for suspended samples (the effective value of α is sensitive to the dielectric properties of the substrate, and is expected to be maximal when the substrate is absent). To date there is no definitive experimental signal for chiral symmetry breaking or mass gap generation; however, non-linearities in the electron dispersion as a result of interactions have been reported in [11]. Even if gap generation does not take place, it is possible that physical graphene lies close to the QCP in the chirally symmetric phase, implying modifications to electron transport.

For the case of a voltage-biased bilayer a new condensation channel, between particles in one layer and holes in the other, opens up; in what follows we will refer to this as "excitonic" condensation. Because of the increasing density of states, as the Fermi energy is raised this should become the preferred channel even though inter-layer interactions are weaker than intra-layer ones. Once again, gap formation results implying an insulating phase; since this can be controlled by the external voltage the possibility of graphene-based electronic components arises [12]. A self-consistent treatment however, taking into account the enhanced screening due to $N_f = 4$, finds the resulting gap $\Delta/\mu \sim O(10^{-7})$, suggesting that excitonic condensation will be difficult to achieve experimentally [13].

Our purpose in this paper is to re-examine excitonic condensation in the non-perturbative setting required by the vicinity of a QCP. We will reformulate the lattice model used for the investigation of the QCP in undoped graphene in [9, 14] to include $N_f = 4$ continuum Dirac fermions and a nonzero isospin chemical potential μ to represent the voltage bias. In order to formulate the model with a local interaction on a $2{+}1d$ lattice, the interaction between fermions is forced to have the form of a contact between local charge densities, schematically $(\bar{\psi}\gamma_0\psi)^2$, and hence no long-range Coulombic tail. As argued in [9], we expect that large vacuum polarisation effects make this irrelevant near the QCP (or equivalently in the large N_f limit). The model is presented in detail in Sec. 2. An important and necessary simplification is that inter- and intra-layer interactions between fermions have a common coupling and hence the same stength. Since $\mu \neq 0$ boosts the density of available particle-hole states, we again expect this to become less relevant as μ is increased.

In Sec. 3 we present results from numerical simulation of the model on lattice volumes 32^3 and 48^3. Since it supposedly describes a continuum effective theory in the vicinity of a QCP it is diffcult at this exploratory stage to assign physical units to the simulation results, or even in principle to know the physical anisotropy ratio a_t/a_s. We choose a coupling strength close to the putative QCP for $N_f = 4$; since the strong-coupling limit

is hard to isolate for our formulation [15] this proves to be a non-trivial exercise, and indeed we will see it appears our simulations lie just in the chirally symmetric phase at $\mu = 0$. Next, we introduce $\mu \neq 0$ and monitor the chiral condensate, carrier density and exciton condensate as it is increased. It will be shown that excitonic condensation does indeed take place and that both carrier density and exciton condensate considerably exceed the values expected for free fermions (augmented by a small symmetry-breaking source term), whereas the chiral condensate is suppressed. We discuss our findings in Sec. 4. Although the model is motivated by condensed matter physics, we will argue the results are of wider interest, and yield perhaps the first insight into Fermi surface physics in the presence of genuinely strong interactions.

2 Formulation and Interpretation of the Model

Here we outline the formulation of an effective field theory for the graphene bilayer. Physically, the idea is that there are $N_f = 2$ flavors of relativistic fermion on each monolayer, described by an action in Euclidean metric [16, 8]:

$$S_{\text{mono}} = \sum_{a=1,2} \int dx_0 d^2x (\bar{\psi}_a \gamma_0 \partial_0 \psi_a + v_F \bar{\psi}_a \vec{\gamma}.\vec{\nabla} \psi_a + i A_0 \bar{\psi}_a \gamma_0 \psi_a) + \frac{1}{2e^2} \int dx_0 d^3x (\partial_i A_0)^2, \tag{1}$$

where e is the effective electron charge (whose value depends on the dielectric properties of the substrate), and the 4×4 Dirac matrices satisfy $\{\gamma_\mu, \gamma_\nu\} = 2\delta_{\mu\nu}$, $\mu = 0, 1, 2$. Note that for this reducible represention of the Dirac algrebra there exist two independent matrices γ_3 and $\gamma_5 \equiv \gamma_0\gamma_1\gamma_2\gamma_3$ which anticommute with the γ-matrices present in (1). A_0 is a fluctuating $3+1d$ electrostatic potential field sourced by the charge density $\bar{\psi}\gamma_0\psi$, and is a remnant of the full electromagnetic field in the instantaneous approximation justified for $v_F \ll c$.

Now, for a perfect bilayer formed from two monolayers stacked in AB configuration with interlayer coupling strength $t' \sim O(0.1)t$ where t is the hopping parameter in the monolayer tight-binding Hamiltonian, it is known that the dispersion relation for massless fermions in the low-energy limit in the vicinity of the Dirac point is quadratic, only becoming approximately relativistic (i.e. linear) for $ka \gtrsim t'/t$ [17]. For $\mu \gg t$ the dispersion then takes the expected form $\varepsilon^2 = (\mu \pm v_F k)^2$ [18]. However, recent theoretical studies of strained bilayers suggest that under mechanical deformation the parabolic bands split to form separate Dirac cones, so that in this case a description in terms of $N_f = 4$ relativistic species is not a bad approximation [19]. Our formulation makes the additional, perhaps unwarranted, approximation that interactions between charge carriers on different layers are of identical strength and character to interactions within a layer - the necessity for this will become clear below.

The second ingredient of the model is that the layers are given equal and opposite constant bias voltages $\pm\mu$, inducing on one layer a negatively charged concentration of particles and on the other a positively-charged concentration of holes. As the notation

implies, the bias voltage is equivalent to a chemical potential, and in fact the theory is formally very similar to the case of QCD with isospin chemical potential $\mu_I = \mu_1 = -\mu_2$, where the subscripts which here label the layers usually stand for the light quark flavors u and d. Euclidean formulations of systems with $\mu \neq 0$ are generally afflicted with a "Sign Problem", ie. the Lagrangian density $\mathcal{L}$ is no longer positive definite, or even real, since the inequivalence under time reversal translates into inequivalence under complex conjugation in Euclidean metric. This makes Monte Carlo importance sampling as a means to handle strongly fluctuating observables inoperable. However, the case of isospin chemical potential is known not to have a Sign Problem and is hence simulable using orthodox methods, as we shall now demonstrate.

If we denote the fermion degrees of freedom on one layer by ψ and on the other by ϕ, define units so that $v_F = 1$, and write $\sum_{\mu=0,1,2} \partial_\mu \gamma_\mu + (iA_0 + \mu)\gamma_0 = D[A;\mu]$, then the fermion part of the Lagrangian can be written:

$$\mathcal{L} = (\bar{\psi}, \bar{\phi}) \begin{pmatrix} D[A;\mu] + m & ij \\ -ij & D[A;-\mu] - m \end{pmatrix} \begin{pmatrix} \psi \\ \phi \end{pmatrix} \equiv \bar{\Psi} \mathcal{M} \Psi \tag{2}$$

Here we have introduced two new real parameters: m is an artificial bare mass which induces a gap in the fermion dispersion relations, and whose sign has no physical consequence for a single flavor in the absence of interactions; j a source strength coupling ψ to ϕ, thus linking the layers and eventually enabling calculation of the exciton condensate. In principle both $m \to 0$ and $j \to 0$ limits need to be taken in order to make contact with physical bilayer graphene. Integration over the Grassmann bispinors $\Psi, \bar{\Psi}$ then results in the functional measure $\det\mathcal{M}[A]$.

An important identity which the model inherits from the gauge theory is

$$D^\dagger[A;\mu] = -D[A;-\mu]. \tag{3}$$

It is then straightforward to check (assuming the dimension of D is even) that

$$\det\mathcal{M} = \det[(D+m)(D+m)^\dagger + j^2] > 0, \tag{4}$$

and

$$\mathcal{M}^\dagger\mathcal{M} = \begin{pmatrix} (D+m)^\dagger(D+m) + j^2 & \\ & (D+m)(D+m)^\dagger + j^2 \end{pmatrix}, \tag{5}$$

implying both that

$$\det\mathcal{M}^\dagger\mathcal{M} \equiv \det^2\mathcal{M}, \tag{6}$$

and also that the desired functional measure $\det\mathcal{M}$ results from integrating over bosonic fields Φ starting from a non-local "pseudofermion" Lagrangian

$$\mathcal{L}_{pf} = \Phi^\dagger[(D+m)^\dagger(D+m) + j^2]^{-1}\Phi. \tag{7}$$

This has the practical advantage that Φ has half as many degrees of freedom as Ψ, and makes eqn. (7) the appropriate starting point for the design of a hybrid Monte Carlo simulation algorithm.

The specific version of $D+m$ in our lattice model employs single-component staggered fermion fields ψ_x, ϕ_x defined on the sites of a $2+1d$ square lattice, with a *non-compact* formulation of the electrostatic potential A_x formally defined on the link joining sites x and $x+\hat{0}$:

$$(D+m)_{xy} = \sum_{i=1,2} \frac{\eta_{ix}}{2}[\delta_{y,x+\hat{\imath}} - \delta_{y,x-\hat{\imath}}] + \frac{\eta_{0x}}{2}[(1+iA_x)e^{\mu}\delta_{y,x+\hat{0}} - (1-iA_{x-\hat{0}})e^{-\mu}\delta_{y,x-\hat{0}}] + m\delta_{xy}, \tag{8}$$

where the signs $\eta_{\mu x} = (-1)^{x_0+\cdots+x_{\mu-1}}$ ensure Lorentz covariance in the long wavelength limit. It can be shown that the relation between the number of staggered fields N (counting ψ,ϕ yields $N=2$) and the number N_f of continuum Dirac 4-spinors is [20]

$$N_f = 2N. \tag{9}$$

It is worth noting the global symmetries present in the model. For $\mu = m = j = 0$ the continuum action (2) is invariant under a U(8) rotation $\Psi \mapsto U\Psi$, $\tilde{\Psi} \mapsto \tilde{\Psi}U^{\dagger}$ where $\tilde{\Psi} \equiv i\bar{\Psi}\gamma_3\gamma_5$. This symmetry is broken to $(\mathrm{U}(4))^2$ by $\mu \neq 0$, and then to $(\mathrm{U}(2))^4$ by $m \neq 0$. Setting the interlayer coupling $j \neq 0$ with $m = 0$ locks the ψ and ϕ components together, so that in this case the residual symmetry is U(4). For the staggered lattice fermions of (8) the original symmetry is $\mathrm{U}(2)\otimes\mathrm{U}(2)_{\varepsilon}$, where the second rotation can be written as $U(\alpha;x) = \exp(i\varepsilon_x\alpha^a\Lambda^a)$, where Λ^a is one of the four hermitian generators of U(2) and $\varepsilon_x \equiv (-1)^{x_0+x_1+x_2}$. Setting $\mu \neq 0$ breaks this to $(\mathrm{U}(1)\otimes\mathrm{U}(1)_{\varepsilon})^2$, followed by $m \neq 0, j = 0$ to $(\mathrm{U}(1))^2$, and $m = 0, j \neq 0$ to $\mathrm{U}(1)\otimes\mathrm{U}(1)_{\varepsilon}$.

The fermion action is supplemented by a Gaussian weight for the A fields:

$$S_{\mathrm{aux}} = \frac{N}{4g^2}\sum_x A_x^2, \tag{10}$$

where g^2 is a parameter governing the strength of the coupling between the potential and the fermions. The resulting dynamics describes A fluctuations having the same form as the continuum action (1) in the strong-coupling or large-N_f limits, but for which explicit screening removes the long-ranged r^{-1} tail away from these limits; further justification for this approximation is given in [9, 14]. For $N_f = 2$ this formulation yields an identical path integral to the lattice action couched in terms of compact link variables given in Eqn. (7) of [14]. For $N_f > 2$, however, the two approaches are not equivalent since the compact formulation leads to extra terms of the form $(\bar{\psi}\psi\bar{\phi}\phi)^2$ in the effective action – although these operators may well be irrelevant at the critical point. The exact lattice version of the non-compact action for $\mu = 0$ and arbitrary N_f once A is integrated out is given in eqn. (2.2) of [21].

We next discuss the implications of relaxing the requirement that inter- and intralayer interactions between fermions are identical. The non-trival terms in the action are of the form $\bar{\psi}Ue^{\mu}\psi$, $\bar{\psi}U^*e^{-\mu}\psi$, where U is a complex number *not* constrained to have unit modulus. Integration over U leads to repulsive particle-particle and hole-hole interactions, and attractive particle-hole interactions. Suppose we wanted to make the model

more realistic by introducing a distinction between intralayer and interlayer interactions. One way to do this would be to introduce a second boson field coupling to ψ and ϕ with opposite signs, in effect introducing repulsion between ψ-particles and ϕ-holes so that the $\bar{\psi}$-ϕ and $\bar{\phi}$-ψ couplings are weaker than those of $\bar{\psi}$-ψ or $\bar{\phi}$-ϕ. The interaction terms could then be written $\bar{\psi}_x UV e^{\mu}\psi_{x+\hat{0}}$, $\bar{\phi}_x UV^* e^{-\mu}\phi_{x+\hat{0}}$, $-\bar{\psi}_x U^* V^* e^{-\mu}\psi_{x-\hat{0}}$, $-\bar{\phi}_x U^* V e^{\mu}\phi_{x-\hat{0}}$, etc. In the limit $V \to 1$ integration over $\psi, \bar{\psi}$ leads to a factor $\det D[\mu]$, while integration over $\phi, \bar{\phi}$ gives $\det D[-\mu]$. With the help of (3) we confirm the resulting functional measure $\det D[\mu] D^\dagger[\mu]$ is positive definite. In the limit $U \to 1$, however, the same process leads to $\det D[\mu] D^*[-\mu] = \det^2 D[\mu]$, which is no longer positive definite. In other words, attempting to make the model more realistic reintroduces a Sign Problem, although a more detailed study would be needed to determine its severity.

Now let's discuss observables. The usual chiral condensate (which has been called the "exciton condensate" in our earlier work [9, 14]) is given by

$$\langle \bar{\Psi}\Psi \rangle \equiv \frac{\partial \ln \mathcal{Z}}{\partial m} = \langle \bar{\psi}\psi \rangle - \langle \bar{\phi}\phi \rangle. \tag{11}$$

Note the sign of the condensate is not physical, and that the two terms on the RHS of (11) give equal contributions. From the discussion above it should be clear that for $\mu \neq 0$ formation of this condensate spontaneously breaks $(\mathrm{U}(1)\otimes\mathrm{U}(1)_\varepsilon)^2$ to $(\mathrm{U}(1))^2$, resulting in two Goldstone modes in the limit $m \to 0$, $j \to 0$. The exciton condensate discussed in [13] and which is the main focus of this paper is given by

$$\langle \Psi\Psi \rangle \equiv \frac{\partial \ln \mathcal{Z}}{\partial j} = i\langle \bar{\psi}\phi - \bar{\phi}\psi \rangle. \tag{12}$$

In this case the symmetry breaks to $\mathrm{U}(1)\otimes\mathrm{U}(1)_\varepsilon$ implying the same number of Goldstones. In fact for $\mu = 0$ and $m = j$, $\langle \bar{\Psi}\Psi \rangle$ and $\langle \Psi\Psi \rangle$ are physically indistinguishable, both being equivalent to the chiral condensate of the $N_f = 2$ theory. Figure 1 below confirms that with $\mu = 0$ our code generates results consistent with $\langle \bar{\Psi}\Psi \rangle / \langle \Psi\Psi \rangle \equiv \frac{m}{j}$.

With $\mu \neq 0$ we next define the charge carrier density

$$n_c \equiv \frac{\partial \ln \mathcal{Z}}{\partial \mu} = \langle \bar{\psi} D_0 \psi \rangle - \langle \bar{\phi} D_0 \phi \rangle. \tag{13}$$

Once again, both terms on the RHS give equal contributions – the first term represents the density of electrons in layer 1, and the second the density of holes in layer 2.

Figure 1 shows the results of a pilot run on 8^3 at $g^{-2} = 0.4$ and $ma = 0.05$. For $ja = 0.05$ the two condensates are degenerate at $\mu = 0$ as argued above. As μ increases, our naive expectation is that a Fermi surface of radius μ forms on each layer, one containing particles, the other holes, implying $n_c \propto \mu^2$. As μ grows, $\psi\bar{\psi}$ and $\phi\bar{\phi}$ pairing are suppressed because a free particle-hole pair costs energy 2μ to create at either Fermi surface, whereas $\psi\bar{\phi}$ pairing is promoted, because it costs zero energy to create a particle on one Fermi surface and a hole at the other, with the density of states at either increasing $\propto \mu$. Thus $\langle \bar{\Psi}\Psi \rangle$ decreases as μ rises from 0, while $\langle \Psi\Psi \rangle$ increases. The rise in $\langle \Psi\Psi \rangle$

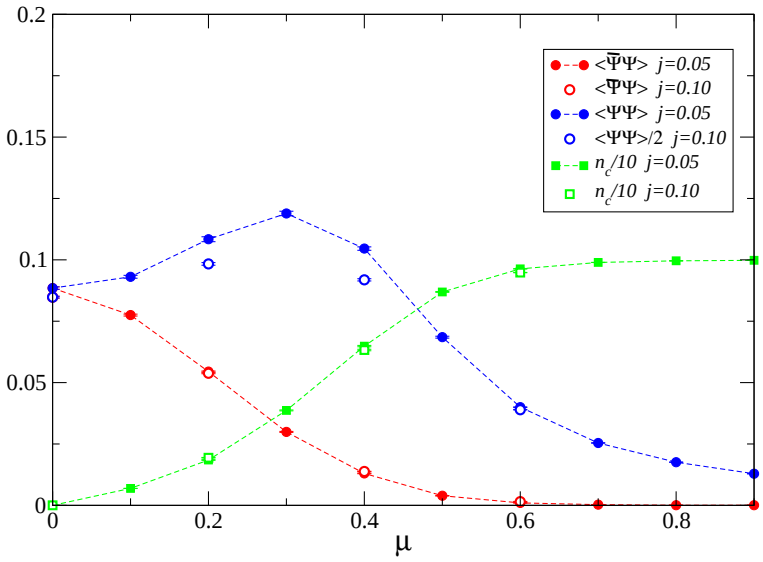


Figure 1: Fermion condensates as a function of μ at $g^{-2} = 0.4$ on 8^3 with bare mass $ma = 0.05$, $ja = 0.05, 0.1$.

seems to be relatively more pronounced for smaller j. This trend persists until $\mu a_t \simeq 0.3$. What happens after that should be understood in terms of *saturation*, an artifact which sets in when the fermion density is a significant fraction of its maximal value of one per lattice site. With our normalisation of n_c this sets in for $\mu a_t \simeq 0.5$, a surprisingly small value based on experience with other models. In a saturated world fermion excitations of all kinds are kinematically suppressed, and the condensates tend to zero in this limit.

3 Numerical Results

Our strategy in this paper is to investigate the effect of varying μ in our bilayer model (8,10) starting close to the quantum critical point. The first task is to find the coupling g_c^2 where the QCP is located for $N_f = 4$; we use the approach [15, 9] of searching for a maximum of $\langle\bar{\Psi}\Psi\rangle$ as g^{-2} is varied and identifying that with the strong coupling limit of the continuum model. We then assume $g_c^{-2} \gtrsim g^{-2}_{\rm peak}$, since if the value $N_{fc} = 4.8(2)$ obtained in [9] is universal there should only be a narrow range of g^{-2} corresponding to the chirally broken phase. The results for $\langle\bar{\Psi}\Psi(m)\rangle$ in Fig. 2 show that $g^{-2}_{\rm peak} \approx 0.30$, much larger than the value ≈ 0.05 obtained with the compact formulation [9]. Another contrast with previous work is that it is also apparent that $g^{-2}_{\rm peak}$ increases with m, from roughly 0.275 at $ma = 0.07$ to 0.35 for $ma = 0.01$, although at this stage we cannot exclude the possibility that finite volume effects influence the result. For small m a linear extrapolation to the chiral limit seems reasonable; we conclude, conservatively, that in this limit $g^{-2}_{\rm peak} \in (0.275, 0.35)$.

Figure 3 shows $\langle\bar{\Psi}\Psi\rangle$ data as a function of m for $g^{-2} \approx g^{-2}_{\rm peak}$. Whilst the quadratic

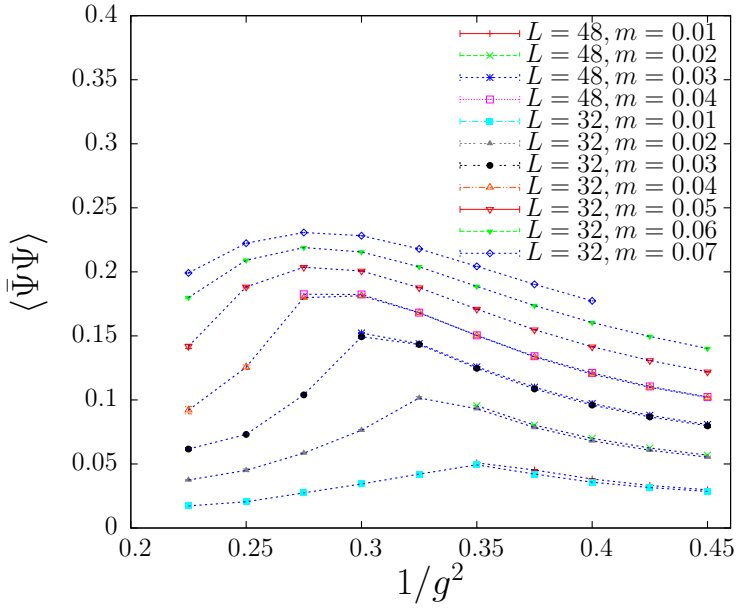


Figure 2: (Color online) $\langle \bar{\Psi}\Psi \rangle$ vs g^{-2} for $N_f = 4$ and various m near $g^{-2}_{\text{peak}} \approx 0.30$. The simulations were performed on both 32^3 and 48^3 lattices.

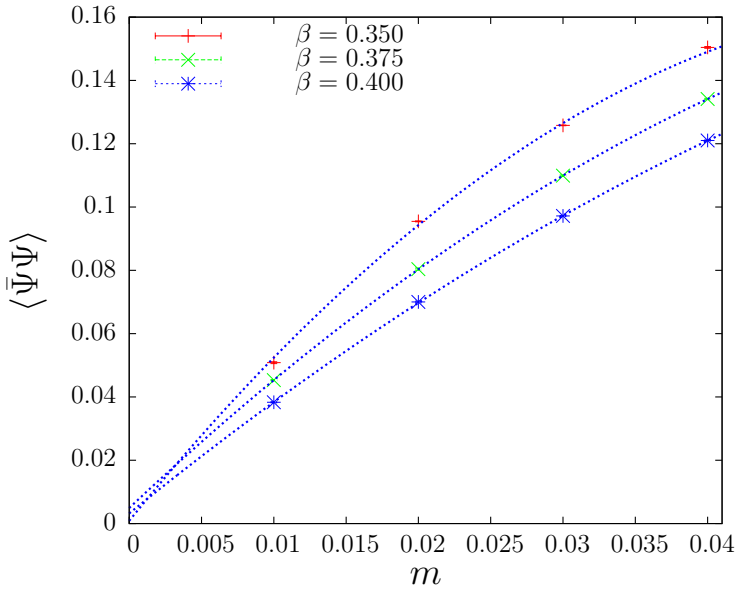


Figure 3: (Color online) $\langle \bar{\Psi}\Psi \rangle$ vs m for $g^{-2} = 0.35, 0.375, 0.40$ fitted to a quadratic polynomial.

extrapolation to the chiral limit is not conclusive, the marked non-linearity of the fits suggests the QCP value g_c^{-2} lies close to this region; however, a much more extensive simulation campaign would be needed to pin it down. For our purposes it suffices to work close to a strongly-interacting QCP, while leaving the issue of whether chiral symmetry spontaneously breaks unresolved. Henceforth, all numerical results are obtained with

the coupling value $g^{-2} = 0.4$ – this implies that the lattice cutoff is constant as μ is varied. Unless otherwise stated, the chiral limit $m = 0$ will be assumed.

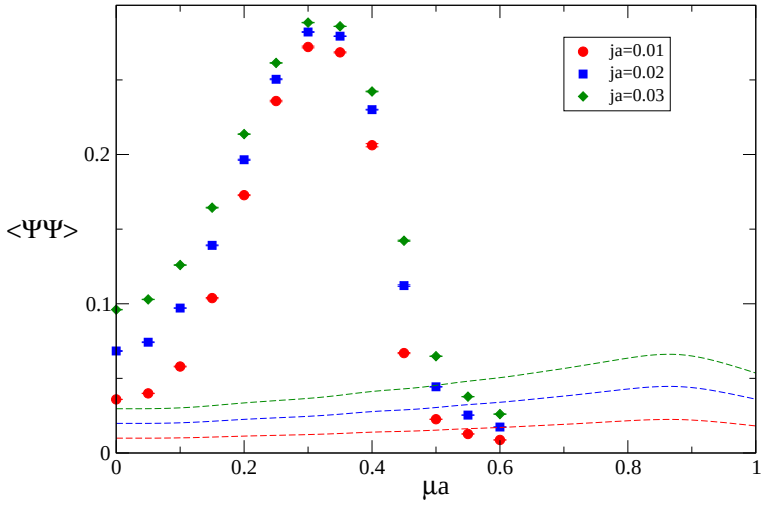


Figure 4: (Color online) $\langle\Psi\Psi\rangle$ vs μ on 32^3 for $m = 0$ and $ja = 0.01, 0.02, 0.03$. Dashed lines show the same quantity evaluated for free fields.

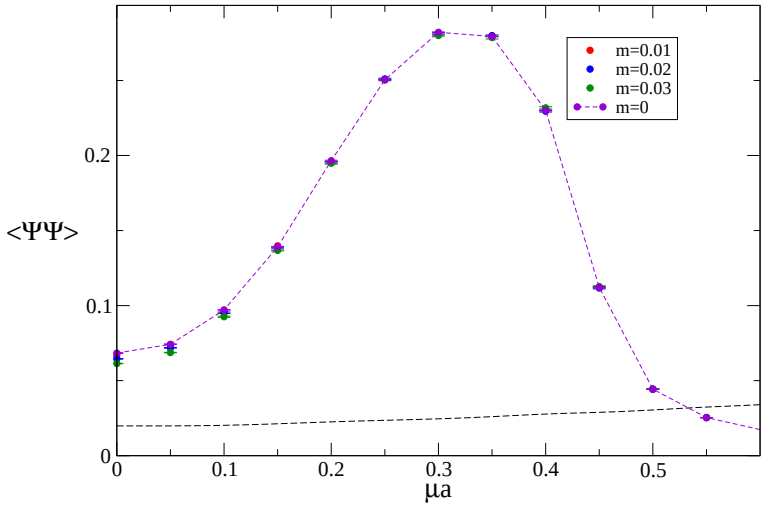


Figure 5: (Color online) $\langle\Psi\Psi\rangle$ vs μ on 32^3 for $ja = 0.02$ and $ma = 0, 0.01, 0.02, 0.03$. The dashed line shows the same quantity evaluated for $m = 0$ for free fields.

Figure 4 shows the exciton condensate $\langle\Psi\Psi\rangle$ as a function of μ for three different j. The figure shows the same broad features as Fig. 1, namely a rapid rise to a fairly sharp maximum at $\mu a \approx 0.3$, followed by a still more rapid fall; the signal is very small indeed by $\mu a = 0.6$. As we shall see in Fig. 8, at this value of μ the system has reached saturation with a maximum possible density of particle-hole pairs consistent with the Pauli exclusion principle on a fixed lattice; our model can only be interpreted as a description of bilayer graphene for values of μ much smaller than this.

The dashed lines in Fig. 4 show $\langle\Psi\Psi\rangle$ evaluated using the same measurement code but with g^2 set to zero, yielding the value for free fields. Since the $(\mathrm{U}(1)\otimes\mathrm{U}(1)_\varepsilon)^2$ symmetry is manifest for $j = 0$ the free-field condensate must vanish in this limit, and the curves are consistent with this expectation. The large disparity between $\langle\Psi\Psi\rangle_{\rm int}$ and $\langle\Psi\Psi\rangle_{\rm free}$ notable in the range $0.2 \lesssim \mu a \lesssim 0.4$ signals that $(\mathrm{U}(1)\otimes\mathrm{U}(1)_\varepsilon)^2$ is surely spontaneously broken here. Close inspection of the figure reveals that $\langle\Psi\Psi\rangle_{\rm free}$ rises monotonically, but not quite smoothly, with μ until reaching a maximum at $\mu a \lesssim 0.9$. The disparity with the apparent saturation observed in the interacting model will be further discussed below. The barely visible wiggles are probably a finite volume artifact similar to that noted in studies of another system with a Fermi surface [3]. Figure 5 plots the same scan but this time showing that the effect of varying m is negligible except for the very smallest values of μ. Since the operator $\Psi\Psi$ is constructed to be conjugate to j, not m, this is as expected.

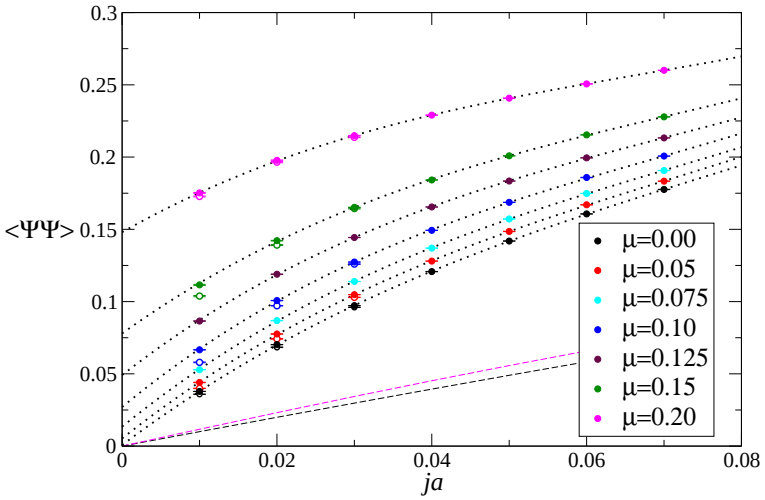


Figure 6: (Color online) $\langle\Psi\Psi\rangle$ vs j for $m = 0$ and various μ on 32^3 (open) and 48^3 (closed symbols). Dotted lines show fits to eqn. (14). Dashed lines show the same quantities evaluated for $\mu = 0, 0.2$ on 48^3 for free fields.

In order to interpret the condensate data it is necessary to extrapolate $j \to 0$. Figure 6 shows $\langle\Psi\Psi\rangle$ for several j on two different volumes, together with extrapolations of the form

$$\langle\Psi\Psi\rangle = \langle\Psi\Psi(j=0)\rangle + Aj + Bj^2 + Cj^3. \tag{14}$$

Taking finite volume effects into account, it seems that at least for $\mu a \geq 0.10$ the fitted intercept is non-vanishing, confirming the spontaneous breaking of particle-hole symmetry due to excitonic condensation $\langle\Psi\Psi\rangle \neq 0$. The extrapolated condensate is shown fitted to a power law of the form $\langle\Psi\Psi(j=0)\rangle = a_1\mu^{a_2}$ in Fig. 7: the fitted parameters are

$$a_1 = 7.0(2); \quad a_2 = 2.39(2). \tag{15}$$

The power-law rise is more rapid than would be expected from a BCS-style mechanism driven by condensation of particle-hole pairs in the immediate vicinity of a Fermi surface.

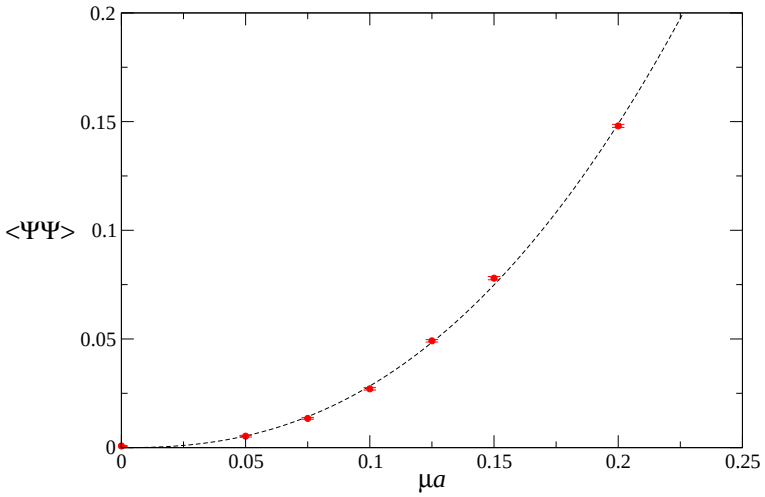


Figure 7: (Color online) $\langle \Psi\Psi(j=0)\rangle$ vs μ on 48^3 fitted to a power law for $\mu = 0.05 - 0.20$. The dashed line corresponds to exponent $a_2 = 2.39(2)$.

This is because in a BCS condensation the density of available pairing states scales with the area of the Fermi surface, $\propto \mu^{d-1}$ in d space dimensions. Despite this somewhat empirical approach, the non-linear increase of $\langle \Psi\Psi\rangle$ with μ is a robust conclusion at variance with a conventional weakly-interacting BCS scenario.

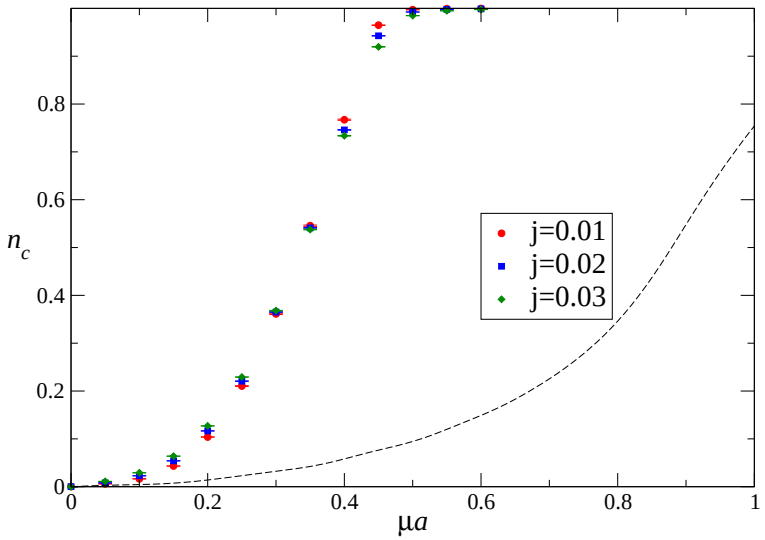


Figure 8: (Color online) Carrier density n_c vs μ on 32^3, $m = 0$ and $j = 0.01, 0.02, 0.03$. The dashed line shows the same quantity evaluated with $j = 0.01$ for free fields.

Next we consider the carrier density n_c defined in (13), and shown in Fig. 8. This rises monotonically from zero with μ until $\mu a \sim 0.5$, when saturation sets in; the effect of $j \neq 0$ is to round off this behaviour by reducing the carrier susceptibility $|\partial n_c/\partial\mu|$ slightly. Once again, the contrast with the free-field behaviour, which only reaches saturation at $\mu a \approx 1.3$ and is shown by the dashed line, is marked.

How should we interpret the finding that $n_c^{\rm int} \gg n_c^{\rm free}$? For degenerate fermions the carrier density, remembering to count both particle and hole states, is given by $n_c = k_F^2/2\pi$. For free massless fermions the Fermi energy μ is equal to Fermi momentum k_F; If we wish to retain the notion of a Fermi surface (albeit one distorted by exciton condensation) for the interacting system, we are forced to conclude $\mu \approx E_F < k_F$ implying strong self-binding, i.e. the degenerate fermions have a large negative contribution to their bulk energy. This is a feature of working near a QCP, and was not observed, e.g. in studies of relatively weakly-interacting systems at non-zero density such as the Gross-Neveu model in 2+1d [22] where interactions are suppressed by $1/N_f$, or two color QCD [4] where the quark density $n_q \gtrsim n_q^{\rm free}$ all the way to saturation.

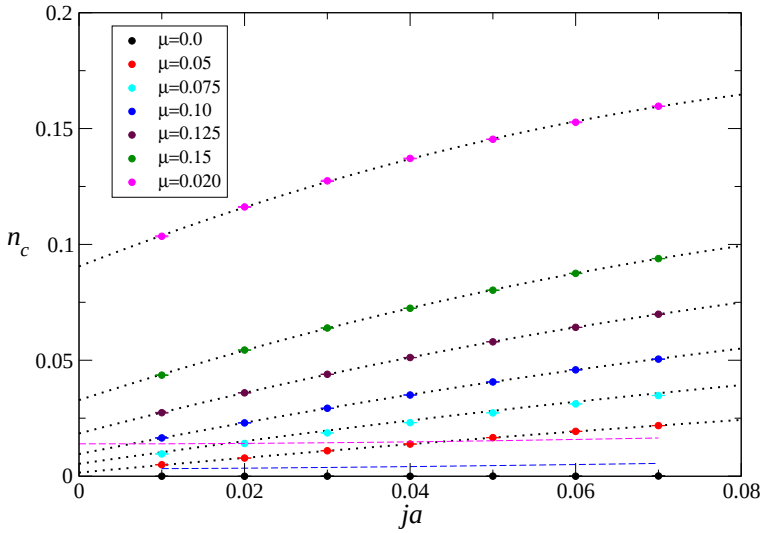


Figure 9: (Color online) Carrier density n_c vs j on 48^3 for various μ. Dotted lines show a quadratic extrapolation $j \to 0$. Dashed lines show the same quantity evaluated for free fields with $\mu = 0.1, 0.2$.

As before, the region of physical interest is for μ well below saturation: Figure 9 plots the variation of n_c with source strength j, togther with a quadratic extrapolation to $j = 0$, showing that the effect of $j \neq 0$ for this observable is regular but certainly not negligible. Finally Fig. 10 plots $n_c(\mu; j = 0)$ together with a power law fit $n_c = b_1 \mu^{b_2}$. The fitted parameters are

$$b_1 = 18.6(4); \qquad b_2 = 3.32(1). \tag{16}$$

As expected, the fitted value of b_2 considerably exceeds the naive expectation $n_c \propto \mu^d$ based on a weakly-interacting system.

In Fig. 11 we show the chiral condensate order parameter $\langle \bar{\Psi}\Psi \rangle$ as a function of μ for various values of the symmetry breaking parameter m at fixed $ja = 0.02$. Its magnitude at $\mu = 0$ falls approximately linearly with m implying restoration of chiral symmetry as $m \to 0$. Even so, it exceeds the free-field value by over a factor of two, reflecting the vicinity of the QCP. Note though that $|\langle \bar{\Psi}\Psi \rangle|$, a measure of the density of particle-hole

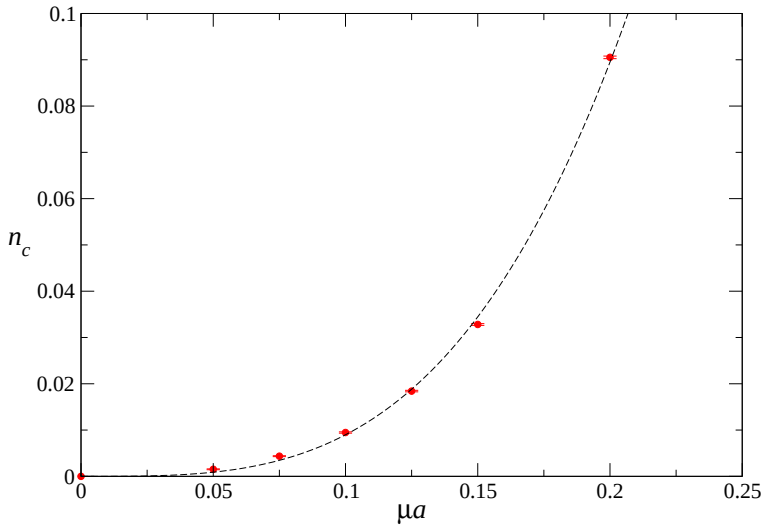


Figure 10: (Color online) Carrier density $n_c(j=0)$ vs μ on 48^3 fitted to a power law for $\mu = 0.05 - 0.20$. The dashed line corresponds to exponent $b_2 = 3.32(1)$.

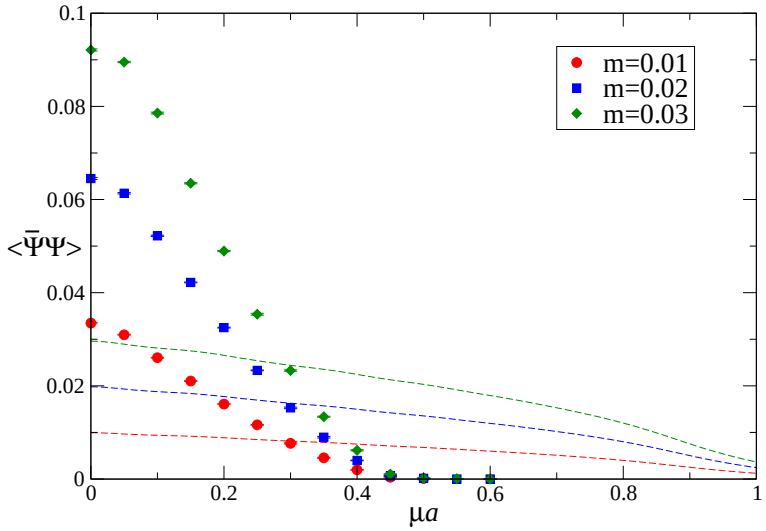


Figure 11: (Color online) Chiral condensate $\langle\bar{\Psi}\Psi\rangle$ vs μ on 32^3 for $j = 0.02$ and $m = 0.01, 0.02, 0.03$. Dashed lines show the same quantity evaluated for free fields.

pairs in the condensate, is roughly one-third of the peak value of the exciton condensate $|\langle\Psi\Psi\rangle|$ seen in Fig. 4. As μ increases $|\langle\bar{\Psi}\Psi\rangle|$ falls monotonically reflecting the increasing difficulty of particle-hole pairing *within* a layer as the biassing voltage rises. We deduce that near the QCP the impact of the biassing voltage is to favour inter-layer over intra-layer pairing; indeed the inter-layer pairing is suppressed completely, falling below even the free-field value, by $\mu a = 0.5$ where saturation sets in.

Finally we report on a preliminary calculation of the spectrum of quasiparticle exci-

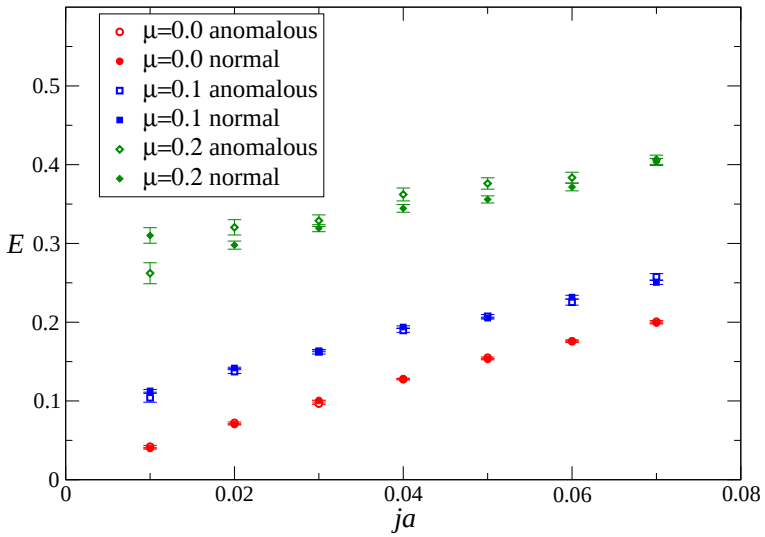


Figure 12: (Color online) Normal and anomalous fermion energies $E(k = 0)$ vs j on 48^3 for $\mu = 0, 0.1, 0.2$.

tations, obtained from analysis of the following fermion correlators:

$$\begin{aligned} C_N(\vec{k},t) &= \sum_{\vec{x}} \langle \psi(\vec{0},0)\bar{\psi}(\vec{x},t)\rangle e^{-i\vec{k}.\vec{x}}; \\ C_A(\vec{k},t) &= \sum_{\vec{x}} \langle \psi(\vec{0},0)\bar{\phi}(\vec{x},t)\rangle e^{-i\vec{k}.\vec{x}}. \end{aligned} \tag{17}$$

Due to the form of the staggered fermion action (8) the set of two-dimensional sites $\vec{x}$ only includes those displaced from the origin by an even number of lattice spacings in any direction, and the physically accessible momenta have $k_i = 2\pi n_i/L_s$ with $n_i = 0, 1, \ldots, L_s/4$. We distinguish between the *normal* propagator C_N describing carrier motion within a layer, and *anomalous* propagator C_A describing inter-layer hopping, which relates eg. destruction of an electron on layer 1 to creation of an anti-hole on layer 2. On a finite system C_A is non-vanishing only for $j \neq 0$.

In this first study we have considered $\vec{k} = \vec{0}$ only. In accordance with a study of quasi-particle propagation in a thin-film BCS superfluid [2] we find that the correlator signal resides in $\mathrm{Re}(C_N)$ and $\mathrm{Im}(C_A)$, and that in the chiral limit $m \to 0$ $C_N(t) \equiv 0$ for t even and $C_A(t) \equiv 0$ for t odd. We thus fit the correlators on every second timeslice for the excitation energy E using the forms

$$\begin{aligned} \mathrm{Re}(C_N(\vec{k},t)) &= Ae^{-Et} + Be^{-E(L_t-t)}; \\ \mathrm{Im}(C_A(\vec{k},t)) &= C(e^{-Et} - e^{-E(L_t-t)}), \end{aligned} \tag{18}$$

where in general $A \neq B$ for $\mu \neq 0$. The resulting energies are shown for small μ as a function of j in Fig. 12. Two features are apparent: firstly normal and anomalous channels yield consistent results, as expected [2], although the normal data have smaller

errorbars; secondly the extrapolation $j \to 0$ appears smooth, and suggests $\lim_{j\to 0} E(j) > 0$ for $\mu \neq 0$. In other words, a voltage bias induces anomalous propagation indicative of particle-hole mixing, a manifestation of excitonic condensation $\langle \Psi\Psi \rangle \neq 0$. This should also result in a non-vanishing energy gap at the Fermi surface, but confirmation requires a study of propagation with $\vec{k} \neq \vec{0}$ [3].

4 Discussion

In this paper we have set out an effective (albeit simplified) field theory for low-energy charge transport in voltage-biased bilayer graphene, and shown how it can be simulated using orthodox lattice field theory methods, because its action in Euclidean metric is real. An interesting feature of the numerical formulation is that it is possible to run in the chiral limit $m = 0$ so long as the $\psi\phi$ coupling $j \neq 0$. There are formal similarities to QCD with non-zero isopsin density [6]; however the resulting dynamics differs sharply. While QCD is an asymptotically-free theory implying that eventually a weakly-coupled description becomes valid as $\mu \to \infty$, here the field correlations remain strong at all scales, even in the absence of confinement, due to the vicinity of the QCP. For this reason the model is of intrinsic theoretical interest independent of any possible physical applications for graphene.

Precise location of the QCP by numerical means has proved challenging; nevertheless the curvature of the chiral condensate data $\langle \bar{\Psi}\Psi(m) \rangle$ of Fig. 3 are suggestive of a critical scaling $\langle \bar{\Psi}\Psi \rangle \propto m^{\frac{1}{\delta}}$ expected at or near a QCP. Equation of state fits predict δ in the range 2.7 (the value for monolayer graphene with $N_f = 2$) [14] to 5.5 (the value in the strong coupling limit $N_f = N_{fc} \approx 4.8(2)$) [9]. Considerably more work would be needed to confirm this quantitatively.

Our main results in this first study are therefore qualitative. Runs with $j \neq 0$ yield measurements of the exciton condensate $\langle \Psi\Psi \rangle$ which show a rapid rise as μ is increased from zero. The data extrapolated to $j \to 0$ suggest that condensate remains non-vanishing in this limit consistent with spontaneous symmetry breaking and superfluidity; indeed the data of Fig. 7 permit a power-law fit $\langle \Psi\Psi \rangle \propto \mu^{2.4}$. This is notable because a weak-coupling BCS description of superfluidity predicts the condensate should scale with the area of the Fermi surface, namely $\langle \Psi\Psi \rangle \propto \mu$. Similarly, the carrier density $n_c \propto \mu^{3.3}$ (Fig. 9), to be contrasted with the weak-coupling behaviour $n_c \propto \mu^2$. With the resolution we are working with there is no sign of an *onset* value of the chemical potential $\mu_o > 0$, such that $n_c = 0$, $\langle \Psi\Psi \rangle = 0$ for $\mu < \mu_o$. This is another important contrast with the systems studied in [1, 2, 3, 4, 5, 6]. The likely reason is that at the couplings studied there is no mechanism for spontaneous mass generation, so that the lightest degree of freedom carrying a conserved charge remains massless. The final interesting observation, shown in Fig. 11, is that the chiral conndensate $\langle \bar{\Psi}\Psi \rangle$ is strongly suppressed as μ rises, presumably because of the rapidly-increasing energy cost of a particle-hole pair *within* a layer, and is consistent with zero post-saturation.

Another observation to note is that below saturation both $n_c \gg n_c^{\rm free}$ and $\langle \Psi\Psi \rangle \gg$

$\langle\Psi\Psi\rangle^{\rm free}$. Once again, this is indicative of strong correlations among the fields, such that $E_F < k_F$, as is the precocious value of μa at which saturation sets in. It suggests that the self-consistent diagrammatic approach of [13] (which employs large-N_f methods so does not probe the QCP) may yield an unduly small estimate of the condensate. It must be stressed, however, that in the absence of a physical scale setting any phenomenogical applications of the model to real graphene are premature.

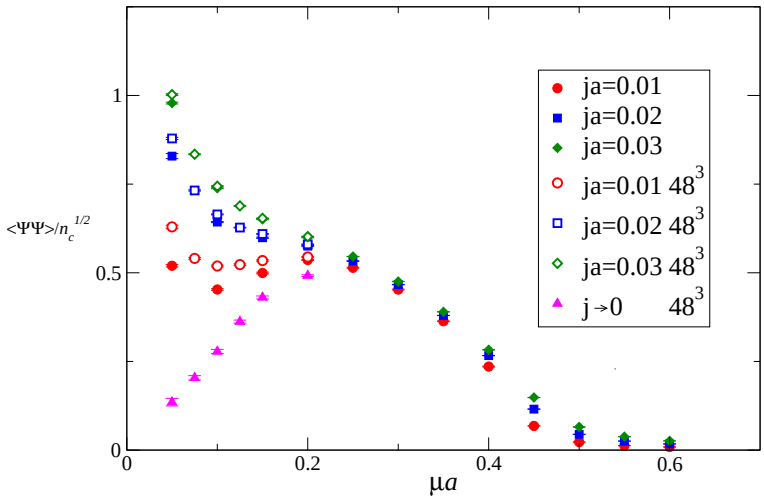


Figure 13: (Color online) The ratio $\langle\Psi\Psi\rangle/n_c^{\frac{1}{2}}$ vs μa on 32^3 (filled) and 48^3 (open) for $ja = 0.01, 0.02, 0.03$, together with the $j \to 0$ extrapolation on 48^3.

In conclusion we claim to have initiated a lattice Monte Carlo study of strongly interacting degenerate fermions, which displays significant qualitative differences to other degenerate systems studied previously. A final question worth discussing is to what extent the concept of a Fermi surface, either sharp or distorted by particle-hole excitonic condensation, remains intact in a strongly-interacting environment. Departures from the canonical weak-coupling are manifested as anomalous scaling with Fermi energy μ (see eqns.(15,16)); however recall that in an interacting Fermi liquid the relation between particle density and Fermi momentum k_F, namely $n_c \propto k_F^d$, should remain inviolate. In the BCS picture, the density of condensed particle-hole pairs $\langle\Psi\Psi\rangle$ arising from plane wave states within a shell of thickness Δ around the Fermi surface implies

$$\langle\Psi\Psi\rangle \propto \Delta k_F^{d-1} \propto \Delta n_c^{\frac{d-1}{d}} . \tag{19}$$

To test whether the scaling (19) is retained even at strong coupling, Fig. 13 plots the ratio $\langle\Psi\Psi\rangle/n_c^{\frac{1}{2}}$ vs. μ for various j on two volumes, together with the $j \to 0$ extrapolation on 48^3. It looks plausible for $\mu a \lesssim 0.2$, on the assumption that the gap Δ has a strong μ-dependence, which should be the case for near-conformal dynamics. It may well prove possible, therefore, to define a Fermi surface in the vicinity of a quantum critical point.

5 Acknowledgements

CPUs used were either Intel(R) Xeon(R) E5420, X5650 or E5-2660. We estimate that over 2 million core hours of computing time were needed to complete this project. The authors wish to thank Diamond Light Source, the Oxford Super Computing Centre (OSC) and the e-Infrastructure South consortium for kindly allowing them to use extensive computing resources, and specifically Tina Friedrich at Diamond Light Source, Luke Raimbach, Lino Garcia Tarres and Steven Young at OSC for help in configuring and maintaining these resources.

References

[1] S. Hands, J.B. Kogut, C.G. Strouthos and T.N. Tran, Phys. Rev. D **68**, 016005 (2003).

[2] S. Hands, B. Lucini and S. Morrison, Phys. Rev. D **65** (2002) 036004.

[3] S. Hands and D.N. Walters, Phys. Lett. B **548** (2002) 196; Phys. Rev. D **69** (2004) 076011.

[4] S. Hands, S. Kim and J.-I. Skullerud, Eur. Phys. J. C **48** (2006) 193;
S. Cotter, P. Giudice, S. Hands and J.-I. Skullerud, arXiv:1210.4496 [hep-lat].

[5] A. Maas, L. von Smekal, B. Wellegehausen and A. Wipf, arXiv:1203.5653 [hep-lat].

[6] J.B. Kogut and D.K. Sinclair, Phys. Rev. D **66**, 034505 (2002).

[7] G. Aarts, Phys. Rev. Lett. **102**, 131601 (2009).

[8] D.T. Son, Phys. Rev. B **75** (2007) 235423.

[9] S.J. Hands and C.G. Strouthos, Phys. Rev. B **78** (2008) 165423.

[10] J.E. Drut and T.A. Lähde, Phys. Rev. Lett. **102** (2009) 026802; Phys. Rev. B **79** (2009) 165425.

[11] D.C. Elias *et al*, Nature Phys. **7** (2011) 701.

[12] E.V. Castro *et al*, J. Phys. Condens. Matter **22** (2010) 175503.

[13] M.Yu. Kharitonov and K.B. Efetov, Semicond. Sci. Technol. **25** (2010) 034004.

[14] W. Armour, S.J. Hands and C.G. Strouthos, Phys. Rev. **B81** (2010) 125105.

[15] S. Christofi, S.J. Hands and C.G. Strouthos, Phys. Rev. D **75** (2007) 101701.

[16] D.V. Khveshchenko, Phys. Rev. Lett. **87** (2001) 246802.

[17] E. McCann and V.I. Fal'ko, Phys. Rev. Lett. **96** (2006) 086805.

[18] A.H. Castro Neto, F. Guinea, N.M.R. Peres, K.S. Novoselov and A.K. Geim, Rev. Mod. Phys. **81** (2009) 109.

[19] M.Mucha-Kruczyński, I.L. Aleiner and V.I. Fal'ko, Phys. Rev. **B84** (2011) 041404(R).

[20] C.J. Burden and A.N. Burkitt, Europhys. Lett. **3** (1987) 545.

[21] L. Del Debbio and S.J. Hands, Nucl. Phys. **B552** (1999) 339.

[22] S. Hands, A. Kocić and J.B. Kogut, Nucl. Phys. B **390** (1993) 355.